

## APPLICATION OF TUNGSTEN OXIDE (WO<sub>3</sub>) CATALYSTS LOADED WITH Ru AND Pt METALS TO REMOVE MTBE FROM CONTAMINATED WATER: A CASE OF LABORATORY-BASED STUDY

*Saleh H. Al-Sharidi, Husin Sitepu & Noktan M. AlYami*

*Research and Development Center, Saudi Aramco, Dhahran, Saudi Arabia*

---

**Received: 01 Jul 2018**

**Accepted: 01 Aug 2018**

**Published: 18 Aug 2018**

---

### ABSTRACT

*The World Health Organization has raised concerns about the accidental fuel leakage during storage and transportation and, therefore extensive methyl tertiary butyl ether (MTBE) use has led to cases of natural water contamination [1-9]. This article describes the (i) visible light reaction condition for MTBE, (ii) solid-phase micro-extraction (SPME) technique incorporated with gas chromatography-mass spectrometry (GC-MS) to assist the MTBE photo-oxidation process, (iii) catalyst syntheses from different concentration of Ru in tungsten oxide (WO<sub>3</sub>), nano-WO<sub>3</sub>, Pt in nano-WO<sub>3</sub>, and (iv) formation of byproducts during photocatalytic degradation of MTBE by using the GC-MS [10-15]. The experimental results indicated that the MTBE removal can quickly and accurately be achieved in presence of Pt-loaded nanostructured WO<sub>3</sub> under visible light radiation, i.e., 96-99% removal between 2.5 hours and 3 hours. The Pt/WO<sub>3</sub> nano-composite showed much better photocatalytic MTBE removal than those of the Ru/WO<sub>3</sub> and pure nanostructured and micron-sized WO<sub>3</sub> [10]. Additionally, the by-products formation during photocatalytic degradation of MTBE obtained from GC-MS revealed that the degradation of MTBE proceeds essentially via formation of formic acid and 1, 1-dimethyl ethyl ester before its complete degradation [10].*

**KEYWORDS:** MTBE, Nano-WO<sub>3</sub>, Ru/WO<sub>3</sub>, Pt/WO<sub>3</sub> Nano-Composite, XRD, GC-MS, UV

### INTRODUCTION

To improve the octane number and increase the gasoline combustion efficiency, methyl tertiary butyl ether (MTBE) as the oxygenated chemical [1-3] has been used by many research groups. Additionally, MBTE has been widely used as a gasoline additive by supplying extra oxygen during the combustion process [1]. Therefore, carbon monoxide and volatile organic carbon emissions from internal combustion engines and air pollution can be reduced. Nevertheless, human and environmental health concerns have raised due to mainly accidental fuel leakage during storage and transportation [4-5]. As a result of leakage, extensive MTBE use has led to cases of water contamination. The United States Environmental Protection Agency (US-EPA) put advisory regulations of 20-40 pp [6-7] for drinking water, and banned MTBE.

MTBE is difficult to treat by air stripping, photo-oxidation, GAC or bio-treatment. There are many research groups proposed a better candidate such as the heterogeneous catalysts combined with photo-oxidation for the removal of MTBE from water resources [1-9]. Seddigi et al. [8] investigated the MTBE photo-catalytically degradation in water by

using semiconducting metal oxides. Using artificial ultraviolet (UV) radiation, they found that both  $\text{TiO}_2$  and  $\text{ZnO}$  were effective photo-catalysts in MTBE remediation. Instead of using the energy source of UV, they developed  $\text{TiO}_2$  and  $\text{ZnO}$  using the visible light in the photocatalytic process. To remove wastewaters containing toxic chemicals, they indicated that a simple single semiconductor catalyst is obviously not effective [10]. Nevertheless, they pointed out that it is a promising result if a doped catalyst [1-9] that works in the visible light is taken with great care [10]. For the degradation of complex molecules, they proposed to use the solar spectrum to measure the photo-catalytic action of the mixed oxide doped photo-catalysts, and obtain the efficiencies of the contaminants' photo catalytic degradation by optimizing the effective photo catalytic reactions parameters. Alfonso-Gordillo et al. [9] indicated that the influent toxicity was significantly reduced after treatment in the packed-bed reactor and, therefore, may be a promising alternative to existing technologies for the removal of MTBE from high-strength MTBE-polluted water [1-9].

In the present study — a case of laboratory-based study, the objectives were to develop (i) visible light reaction condition for MTBE and the SPME technique incorporated with GC-MS to assist the MTBE photo-oxidation study, (ii) catalyst syntheses Ru in  $\text{WO}_3$ , nano- $\text{WO}_3$ , Pt in nano- $\text{WO}_3$ , and the formation of by products during photo catalytic degradation of MTBE by using the GC-MS [10].

## Experimental

To reproduce the results that originally conducted by Sharidi [10], the authors have used his method of sample preparation and are given briefly below.

*MTBE Samples.* Following to Sharidi study [10], in this study the authors prepared MTBE stock solution of 1000 ppb by dissolving 0.00025g of MTBE in 2.0 L of water, and then 100 ml of 1000 ppb MTBE stock solution was added in 1 L to prepare 100 ppb MTBE stock solution that was used for the reaction [10]. The study was utilized a visible light in 500 ml reactor and the lamp introduced an immersion well photochemical reactor made of Pyrex glass equipped with a magnetic stirring bar, a water circulating jacket and an opening for supply of gases. The photo-oxidation experiments preparation and the synthesized catalyst procedures were described by Sharidi [10].

*Synthesizing  $\text{WO}_3$  in sodium tungstate.* Sodium tungstate was dissolved in 100 mL double distilled water (DDW) (6.6 g, 0.2 moles) and acidification was conducted by adding HCl to get a pH of 1 to obtain a white precipitate and dissolve by adding oxalic acid (0.4 g in 30 mL DDW, 0.1 moles) [10]. As a result, a transparent solution was obtained. The solutions were transferred into 100 mL Teflon-lined stainless steel autoclave and maintained at  $180^\circ\text{C}$  for 24 hours to get the final product [10].

*Synthesis of noble metals (Ru/Pt) loaded on  $\text{WO}_3$ .* The authors prepared the photo-deposition of Ru loaded on  $\text{WO}_3$  by 500mg of  $\text{WO}_3$  and placed 100.0 mL of distilled water in a beaker [10]. Then, 2.5mg of Ru was added to the beaker. After that, the solution bubbled with nitrogen for 30 minutes to remove the excess of  $\text{O}_2$  while stirring slowly [10]. Then, added 5.0 mL of methanol. Then, the authors transferred the solution to the reactor and turn the lamp for 6 hours while stirring via a magnetic stirrer and a stirring plate. After the reaction took placed, co-catalyst Ru/ $\text{WO}_3$  centrifuging the solution for 30 minutes and dries the catalyst at  $\sim 700^\circ\text{C}$  in the oven. Similarly, the Pt/ $\text{WO}_3$  was prepared [10]. Following to Sharidi study [10], the procedures used in the present study were to

- assess the treatability of water contaminated by MTBE
- develop visible light reaction condition for MTBE and SPME technique incorporated with GC-MS in assisting the study of MTBE photo-oxidation
- synthesize 0.5 wt% of Ru, 1.0 wt% of Ru, 1.5 wt% of Ru, 2.0 wt% of Ru, and 2.5 wt% of Ru in WO<sub>3</sub>
- synthesize 0.5 wt% of Pt, 1.0 wt% of Pt, 1.5 wt% of Pt, 2.0 wt% of Pt, and 2.5 wt% of Pt in WO<sub>3</sub>
- synthesize 0.5 wt% of Pt, 1.0 wt% of Pt, 1.5 wt% of Pt, 2.0 wt% of Pt, and 2.5 wt% of Pt in nano-WO<sub>3</sub>
- determine MTBE degradation and hydrocarbon by-products from photo-oxidation

*Characterization of the Synthesized Catalysts by X-ray powder diffraction (XRD) [11-14].* The synthesized catalyst powders were manually ground in an agate mortar and a pestle for several minutes to achieve fine particle size and adequate intensity reproducibility [11-14]. Then, the fine powder was mounted into the XRD sample holder by back pressing. Table 1 shows the XRD pattern measurement conditions. The continuous-scanned patterns were measured with a PANalytical X'PERT XRD diffractometer with copper X-ray tube. In this article, the authors used the software package PANalytical High Score Plus (X'Pert High Score Plus Version 2.2c PANalytical Inc.), combined with the International Center for Diffraction Data (ICDD) of the Powder Diffraction File (PDF-4+) database of the standard reference materials [11-14].

**Table 1: XRD Pattern Measurement Condition [11-14]**

Name	Description
Instrument	PANalytical X'PERT PRO MPD
Radiation	Cobalt-anode tube operated at 40 kV and 40 mA Wavelength: K $\alpha_1$ = 1.78901Å, Co K $\alpha_2$ = 1.79290Å, K $\alpha_2$ / K $\alpha_1$ ratio = 0.50
Optics	Bragg-Brentano, measuring circle diameter = 480 mm Divergence slit type: automatic Irradiated length = 10 mm and Specimen length = 10 mm Distance Focus to Divergence Slit = 100 mm
Specimen	Holder: Circular format, diameter = 20 mm Rotation "on" for all measurements
Detector	PSDX' Celerator PSD mode: scanning; PSD length in 2 $\theta$ = 2.12°
Acquisition	Angular range in 2 $\theta$ : 2° - 70° Step size: 0.008° Scanning step time: 9.7282 s

*Microstructural and Compositional Characterization [10].* The Environmental Scanning Electron Microscopy (ESEM) uses electrons instead of visible light to form magnified images of an object by scanning it with a high-energy beam of electrons in a raster scan pattern [10]. It is the natural extension of the conventional SEM and incorporates all of the conventional functions of SEM with additional capabilities. Secondary electron and backscattered electron images along with energy dispersive X-ray spectroscopy system (EDS) spectra were acquired from different parts of the examined samples [10]. The samples were mounted on ESEM stub using double sized conductive carbon tapes and then inserted into the ESEM chamber for examinations [10].

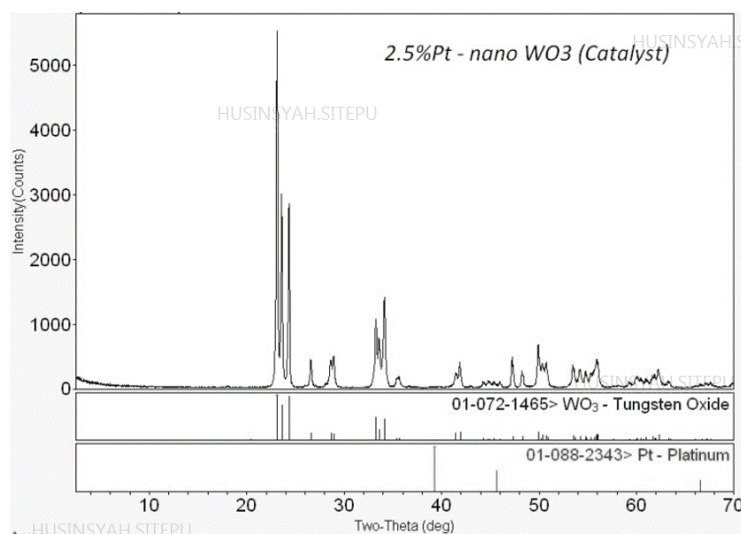
*Photo-Oxidation Reactor [10].* Following the previous study conducted by Sharidi [10], the authors used visible light illumination, the photocatalytic activities of samples were subsequently evaluated in term of the MTBE degradation. The photo-catalyst powder (100 mg) was dispersed and/or added to the reactor containing 100 ml of MTBE stock solution, 100 ppb in concentration [10]. A halogen lamp was placed in the reactor attached to the water flow cooling system. The mixture was stirred gently, samples were taken at different time scales; the first sample (0 minutes) was taken after 30 minutes of constant stirring with the lamp turned off [10]. The lamp was switched on and the second sample was taken after 30 minutes and the other samples were taken after 2 hours (2h), 3h, and 4h, respectively [10].

*GC-MS.* The efficiency of the used catalysts was evaluated by the GC-MS through the use of SPME technique [10], which the SPME was placed in each vial for 10 minutes to collect the vapors of MTBE with great care to keep the fiber above the liquid level. Additionally, it was injected into the GC-MS instrument to obtain the required results with an estimated run time of around 9 minutes for the single analysis [10]. Every sample was run twice to ensure the stability of the results and, then between every run, the fiber was dipped in water and then injected to the GC-MS, thus to make sure that there is no MTBE contamination coming from the previous sample [10].

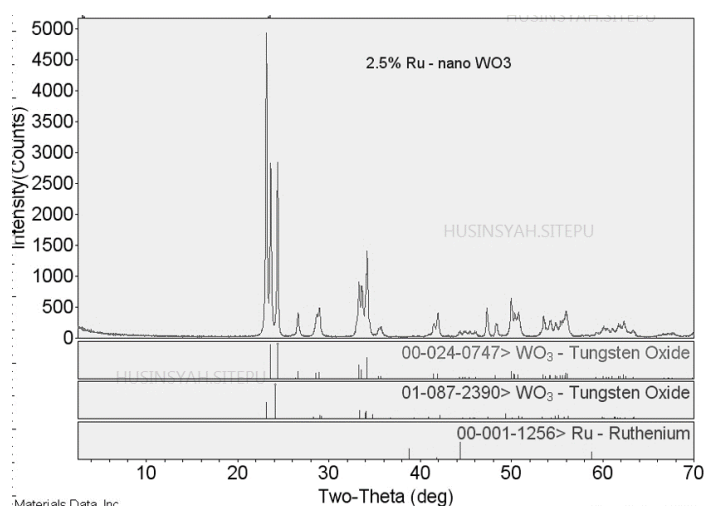
## RESULTS AND DISCUSSIONS

*XRD Phase Identification Results.* XRD analysis was carried out to assess the crystallinity of the synthesized catalyst used in the current study [11]. Figure 1 shows the XRD phase identification results for the (a) 2.5 wt% of Pt in nano-WO<sub>3</sub> and (b) 2.5 wt% of Ru in nano-WO<sub>3</sub> catalyse catalysts. It is clearly seen from Figure 1 that the samples mainly consist of tungsten oxide. The Pt and Ru are not clearly shown in the XRD patterns due to the fact that the starting noble metals are organic materials.

*SEM and EDS Investigation Results.* The ESEM results revealed that the starting WO<sub>3</sub> materials consists of regularly shaped fine particles, see Figure 2(a). Figure 2(b) showed the ESEM andEDS investigation of the synthesized sample and indicated the formation of platelet-like nano-structure of tungsten oxide [10]. Figure 2(c) showed the ESEM analyses of Pt/nano-WO<sub>3</sub> and showed that the formed product comprises regularly shaped nano particles, which agree well with the XRD results [10], see Figure 1.

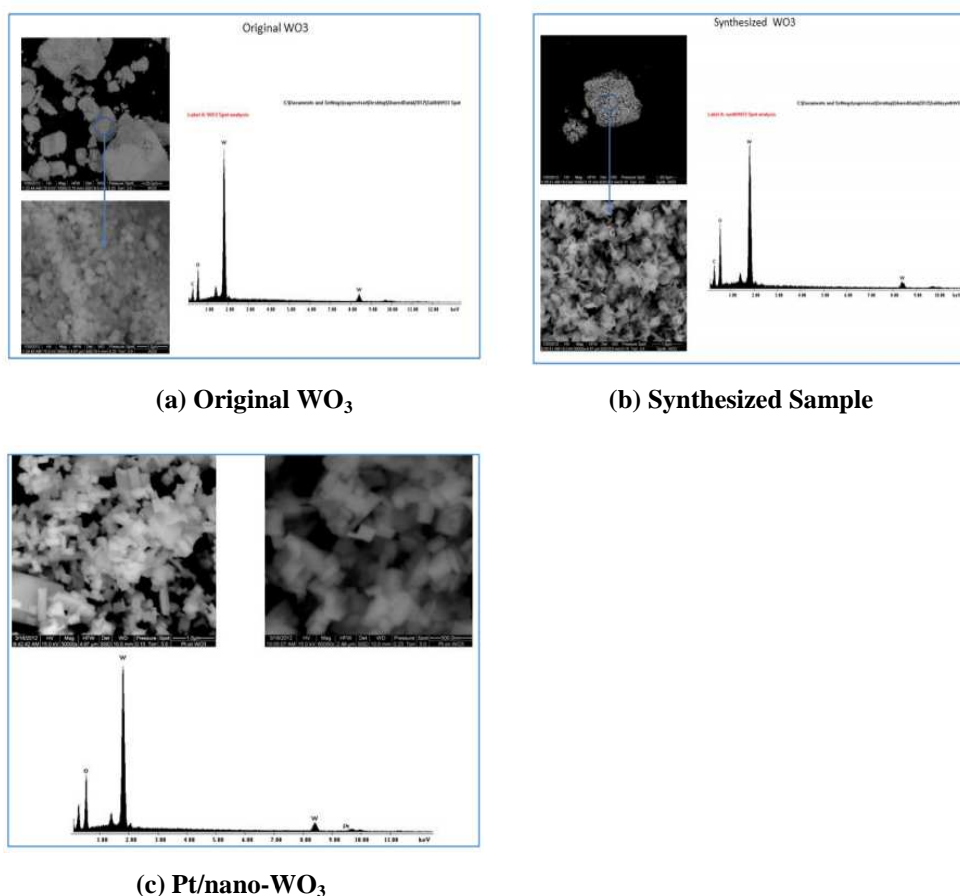


(a) 2.5 wt% of Pt in nano-WO<sub>3</sub> Catalyst



(b) 2.5 wt% of Ru in nano- $WO_3$  Catalyst

Figure 1: XRD Phase Identification Results of the Synthesized (a) 2.5 wt% of Pt in nano- $WO_3$  and (b) 2.5 wt% of Ru in nano- $WO_3$  Catalysts Along with the Reference Patterns of the Identified Compounds



(a) Original  $WO_3$

(b) Synthesized Sample

(c) Pt/nano- $WO_3$

Figure 2: ESEM Images and Corresponding EDS X-Ray Spectra of (a) Original  $WO_3$ , (b) Synthesized Sample and (c) Pt/nano- $WO_3$  Catalysts

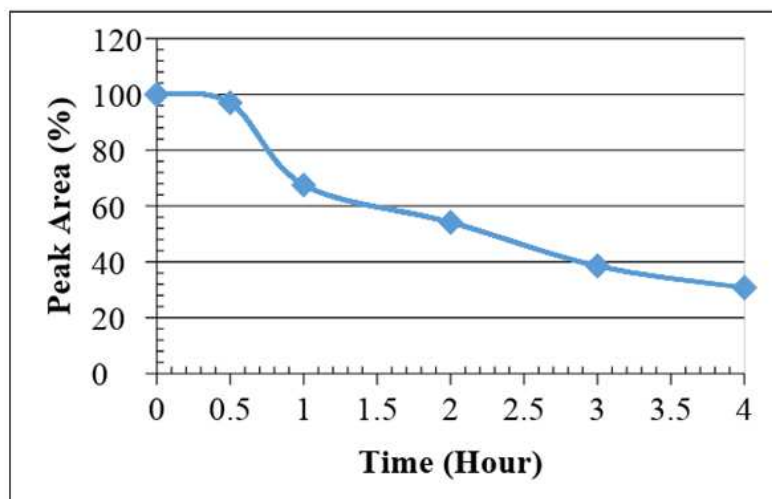


**Figure 3: The Degradation of MTBE via Pure  $WO_3$  Using Halogen Lamp Excitation for 4 hours**

### MTBE Photo-Oxidation

*Pure Tungsten Oxide ( $WO_3$ ).* The authors determined the MTBE photo oxidation by the solid oxide of  $WO_3$  through the halogen lamp excitation for 4h of testing. The catalyst was used about 100 mg in 100 ml stock solution contained 100 ppb MTBE [10]. Figure 3 shows the reduction of MTBE about 69% after 4h of treatment with a relative standard deviation of  $\pm 0.2$ -5.9% [10]. The MTBE was treated by pure  $WO_3$  for the (a) 0 minute, (b) 30 minutes, (c) 1h (d) 2h, (e) 3h and (f) 4h using GC-MS chromatography diagram [10]. The results revealed that a drop in MTBE peak area but no hydrocarbon by-product was detected except MTBE reduction [10].

*MTBE Photo-Oxidation by Ru Loaded with Tungsten Oxide ( $WO_3$ ).* Figure 4 depicts the MTBE degradation via 0.5%, 1.0%, 2.0% and 2.5% of Ru loaded on  $WO_3$  treated by halogen lamp and catalyst weight 100 mg in 100 mL stock solution contained of 100 ppb MTBE [10]. For 4h of treatment, the Ru/ $WO_3$  degraded the MTBE in one systemically trend and the MTBE reduction was ranged from 49% to 79% [10]. The results show that the loading of Ru was not much different for the MTBE reduction compared to those of the pure  $WO_3$  [10]. The GC-MS chromatography diagram of the treated MTBE by 2.5% Ru/ $WO_3$  for the (a) 0 minute, (b) 30 minutes, (c) 1h, (d) 2h, (e) 3h and (f) 4h yielded the loading of Ru, which was not much of a difference in reduction of MTBE when compared to pure  $WO_3$  and, therefore the chromatography of Ru/ $WO_3$  catalysts showed no hydrocarbon by-products formed [10].

*MTBE Photo-Oxidation by Ru Loaded on Nano- $WO_3$ .* Figure 5 depicts the nano- $WO_3$  loaded by Ru catalyst were degraded the MTBE in one systemically trend and the reduction was ranged from 39% to 62% of MTBE for 4h treatment duration [10]. The results revealed that Ru increases, lead to decreases the  $WO_3$  activity and no increase in the MTBE reduction [10]. The treated MTBE by 2.5% Ru/nano  $WO_3$  from 0h to 4h under the halogen lamp, catalyst weight 100 mg in 100 mL stock solution contained 100 ppb MTBE by using the GC-MS chromatography diagram [10]. The results showed that showed neither the degradation of MTBE nor the hydrocarbon by-products [10].

*Photo-Oxidation of MTBE via Pt Loaded on  $WO_3$ .* In this sample preparation section, the authors used the technique that Sharidi [10] employed in his study. The MTBE photo-oxidation was tested by using 0.5, 1.0, 1.5, 2.0 and 2.5% of Pt loaded in  $WO_3$  and, therefore, the photo-oxidation was tested for 4h for each catalyst and the weight of each catalyst was 100 mg in 100 mL stock solution contained 100 ppb MTBE [10]. The Pt-loaded on  $WO_3$  were degraded the

MTBE steeply and increased after 1h to 3h and, then after 4h the MTBE treatment achieved 98% (Figure 6), whereas Figure 8 shows the GC-MS chromatography diagram illustrates the photo-oxidation of 0.5% Pt/WO<sub>3</sub> to MTBE, after 1h the by-product of formic acid 1,1-dimethyl ethyl ester was generated during the oxidation [10]. The by-product was increased as MTBE decreased after 2h of the treatment and, then, at 3h the MTBE reduced more than 90% and the by-product started to decrease as well [10]. The trace level was observed by-product after 4h treatment.

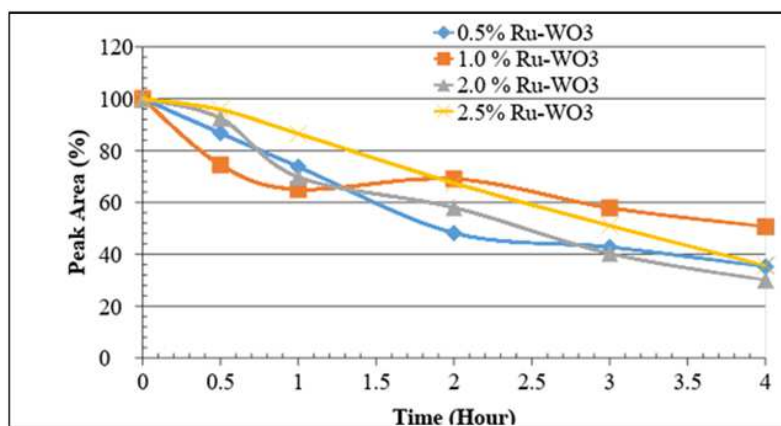


Figure 4: The MTBE Degradation via Different Concentration of Ru Loaded on WO<sub>3</sub>. The Ru/WO<sub>3</sub> Degraded the MTBE in one systemically Trend and the MTBE Reduction was ranged from 49% to 79% for 4h Treatment

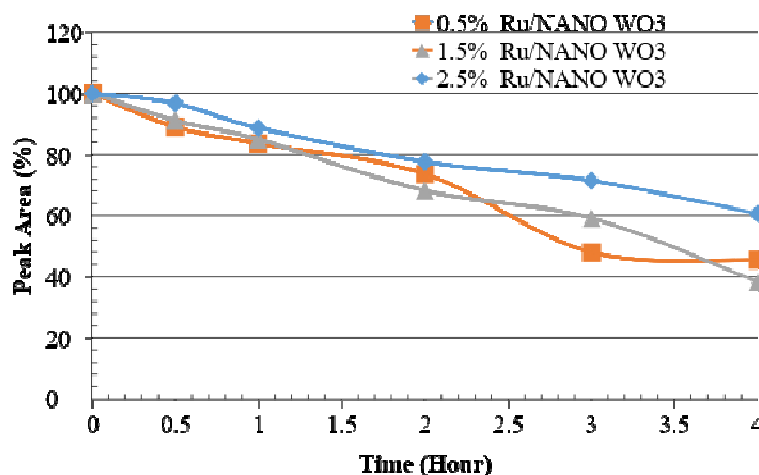


Figure 5: The MTBE Degradation via 0.5%, 1.5% and 2.5% of Ru Loaded on nano WO<sub>3</sub>. The Degradation Ranged from 39 to 62 % of MTBE for 4h Treatment. The Results Indicted Increase of Ru, Lead to a Drop in the Activity of WO<sub>3</sub> but no Increase in the Degradation of MTBE

*MTBE Photo-Oxidation by Pt in Nano-WO<sub>3</sub>* The sample preparation described in this section was taken from Sharidi [10]. The nano WO<sub>3</sub> loaded by Pt for a ratio of 0.5, 1.5 and 2.5% and tested through the MTBE photo-oxidation and, therefore, the experiment was performed with 4h treatment duration for each catalyst, and the weight of each catalyst was 100 mg in 100 mL stock solution contained 100 ppb MTBE [10]. Figure 7 shows the Pt loaded on nano WO<sub>3</sub> achieved MTBE degradation more than 85% after 1h of the treatment and, therefore, the additional three loaded percentage of Pt in nano WO<sub>3</sub> was achieved 99% of MTBE degradation after 3h of the treatment with the trace of by-product [10].

The by-product was effectively reduced from the sample after 3h at Pt/nano WO<sub>3</sub> compared to the photo-oxidation of Pt/WO<sub>3</sub> treatment. Figure 9 depicts the results of 0.5% Pt/nano WO<sub>3</sub>. The GC-MS chromatography was shown the MTBE molecule

- dramatically decrease after 0.5h of treatment and by-product of MTBE produced formic acid 1, 1-dimethyl ethyl ester form the treatment, and has 90,000 peak high,
- started to decrease after 1h of treatment and by-product of MTBE produced formic acid 1, 1-dimethyl ethyl ester form the treatment,
- decreases after 2h of treatment and by-products increases from 24,000 to 29,000 peaks high, and
- Decreases after 3h of treatment and by-products started to decrease to trace amounts [10].

## DISCUSSIONS

The photo-oxidation of pure WO<sub>3</sub> helped to degrade up to 70% of MTBE from contaminated groundwater. Also, Ru loaded on WO<sub>3</sub> and nano-WO<sub>3</sub> did not show improvements in MTBE degradation. Pt loaded on pure WO<sub>3</sub> helped in the degradation of the MTBE 98% within 4h. The authors prepared five active catalysts by using nano-WO<sub>3</sub> and pure WO<sub>3</sub> to compare the photo-oxidation by doping Ru and Pt metals [10].

The pure WO<sub>3</sub> photo-oxidation was gradually achieved process to degrade the MTBE from the contaminated groundwater up to 69%. Nevertheless, the Ru metal had not shown improvement of MTBE photo-oxidation re education catalytically. In addition, the Ru doped in nano-WO<sub>3</sub> catalysts was shown lower activity towered the MTBE degradation. The MTBE demineralization by pure WO<sub>3</sub>, Ru/WO<sub>3</sub>, and Ru/nano-WO<sub>3</sub> was shown not hydrocarbon by-product observed and the completed MTBE photo-oxidation oxidation.

The Pt metal doped in pure WO<sub>3</sub> and nano-WO<sub>3</sub> were shown active photo-oxidation and the MTBE degradation was achieved 95-98% and 99% respectively. The MTBE demineralization by Pt/WO<sub>3</sub> was observed by GC-MS and by-product formic acid 1,1-dimethyl ethyl ester after 0.5h and 1h of treatment. The degradation of both MTBE and by-product was observed dramatically after 3h to 4h. In addition, Pt-doped in nano WO<sub>3</sub> was higher active catalysts and the MTBE reduction photo-oxidation was achieved 99%. The Pt metal doped in WO<sub>3</sub> was shown high oxidation and reaction time due to generating the redox of OH\* and it acts as an oxidizer agent compared to the Ru doped in WO<sub>3</sub>. Additionally, the Pt-doped in nano-WO<sub>3</sub> was shown higher MTBE oxidation compared with Pt-doped in pure WO<sub>3</sub>. The below equation is shown the MTBE demineralization pathway at Pt/WO<sub>3</sub> through visible light photo-oxidation.





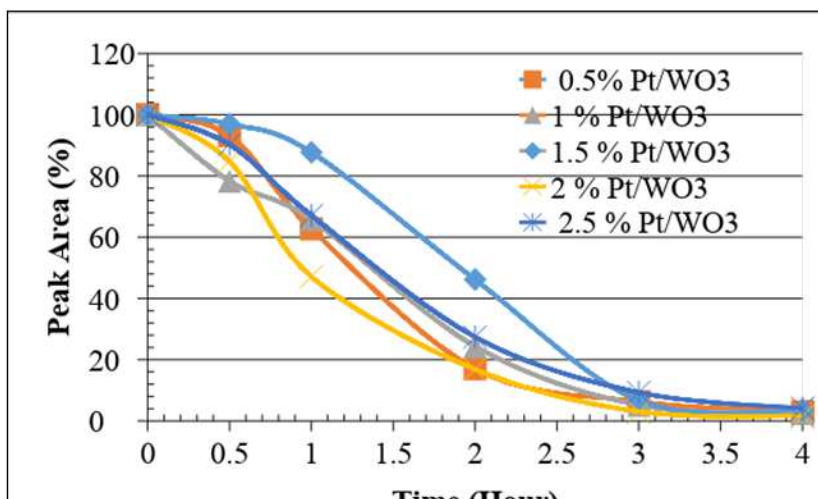


Figure 6: The MTBE Degradation via 0.5, 1.0, 1.5, 2.0 and 2.5% of Pt Loaded on  $WO_3$ . The MTBE Degradation was Very Steep and Degradation Intensified after 1h to 3h and, then after 4h 98% MTBE Degradation was Achieved [10]

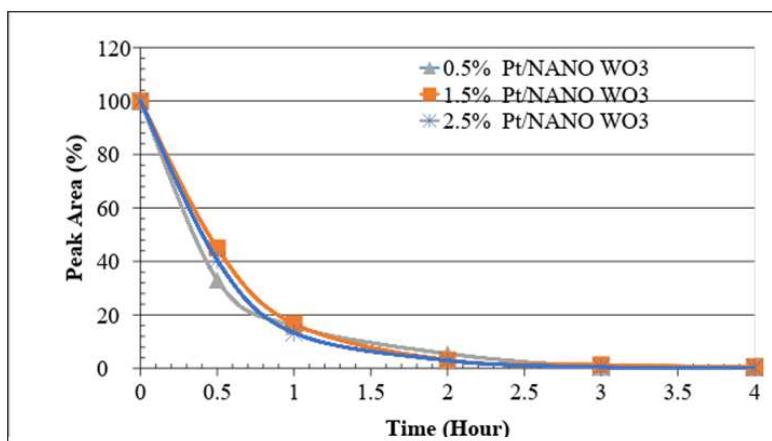
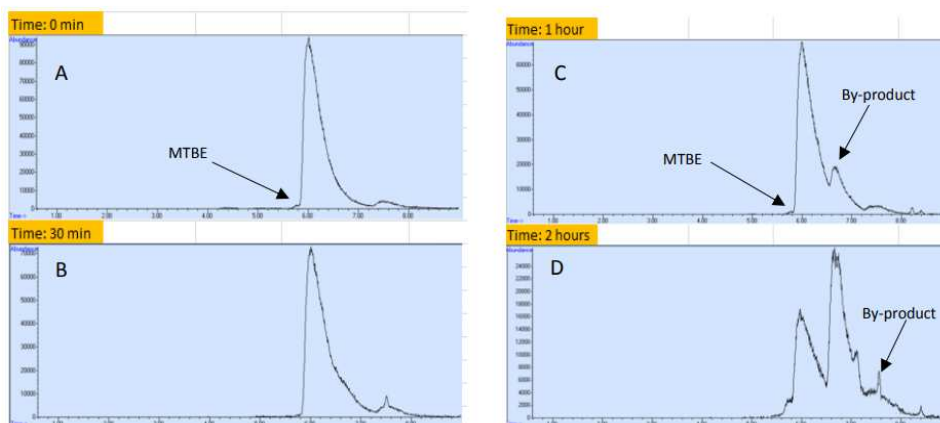
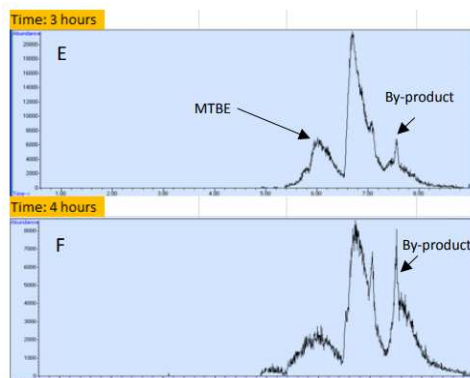


Figure 7: The MTBE Degradation via Different Concentration of Pt Loaded on nano  $WO_3$  Treated By Halogen Lamp with Catalyst weighing 100 mg in 100 mL Stock Solution of 100 ppb MTBE. After three hours of Treatment around 99% Degradation MTBE was Achieved [10]





**Figure 8: The GC-MS Chromatography Diagram of MTBE Treated by 0.5% Pt/WO<sub>3</sub> from 0 min to 4h under the Halogen Lamp [10]**

It can then be highlighted in the findings that the MTBE removal achieved very fast in presence of Pt-loaded nanostructured WO<sub>3</sub> and visible light, i.e., 96-99% between 2.5h and 3h. Additionally, Pt/WO<sub>3</sub> is superior photocatalytic than the Ru/WO<sub>3</sub>, pure nanostructured and micron-sized WO<sub>3</sub> [10]. The GC-MS results showed that the MTBE degradation proceeds essentially via formation of formic acid and 1,1-dimethyl ethyl ester before its complete mineralization [10]. The MTBE degradation achieved up to 99% with traces of by-product through Pt/nano-WO<sub>3</sub> at the visible light condition, and treatability by selected visible light photo-oxidation catalysts was showed. Photo-oxidation over WO<sub>3</sub> and nano-WO<sub>3</sub> was demonstrated, where the visible light treatment was faster and generated HO\* redox agent in Pt-doped nano WO<sub>3</sub> after treatment for 0.5h [10]. Finally, the laboratory synthesis was confirmed by XRD (Figure 1) and the observed mechanism was proposed based on the mass spectroscopy results (Figures 8 and 9). The study achieved 99% treatment of MTBE by using Pt/nano-WO<sub>3</sub> photocatalyst [10].

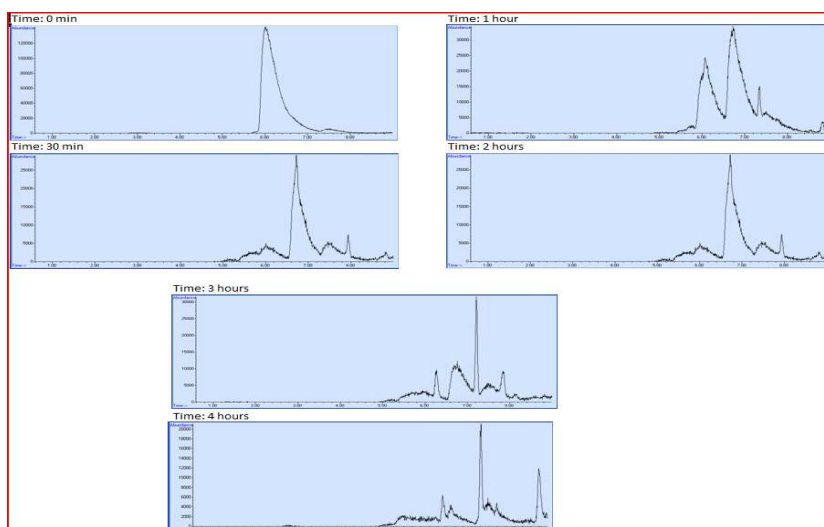


**Figure 9: The Photo-Oxidation Result and the GC-MS Chromatography Diagram for 0.5% Concentration of Pt Catalyst Loaded on nano WO<sub>3</sub>**

## CONCLUSIONS

In the present study, the authors developed visible light reaction condition for MTBE, and used the SPME technique incorporated with GC-MS to investigate the MTBE photo-oxidation process, modified the photo-catalysts surface with platinum (Pt) and ruthenium (Ru) metals and resulting activity of samples were compared and described; and characterized the synthesized catalysts to monitor changes in MTBE degradation, structural, and chemical properties. The experimental results indicated that the MTBE removal can quickly be achieved in presence of Pt-loaded nanostructured WO<sub>3</sub> under visible light radiation, i.e., 96-99% removal between 2.5h and 3h. The Pt/WO<sub>3</sub> nano-composite showed much better photocatalytic MTBE removal than Ru/WO<sub>3</sub> and pure nanostructured and micron-sized WO<sub>3</sub> [10]. Additionally, the by-products formation during photocatalytic MTBE degradation obtained from GC-MS revealed that the degradation of MTBE proceeds essentially via formation of formic acid and 1, 1-dimethyl ethyl ester before its complete degradation [10].

## Conflicts of Interest

The authors declare that there are no conflicts of interest regarding the publication of this paper.

## ACKNOWLEDGMENTS

The authors would like to thank the management of Saudi Aramco for permission to publish this article. The support and encouragement of TSD/R&DC management are acknowledged.

## REFERENCES

1. Z. S. Seddigi, S. A. Ahmed, S. P. Ansari, N. H. Yarkandi, E. Danish, M. D. Y. Oteef, and M. Cohelan, "Photocatalytic Degradation of Methyl tert-Butyl Ether (MTBE): A review," *Adv. Env. Res.*, Vol. 3 No1, pp. 11-28, 2014.
2. M. N. Siddiqui, and Gondal, M. A., "Nanocatalyst support of laser-induced photocatalytic degradation of MTBE," *J. Environ. Sci.* Vol 49, pp. 52-58, 2014.
3. R. L. Zhang, G. Q. Huang, J. Y. Lian, and X. G. Li, "Degradation of MBTE and TBA by a new isolate from MTBE-contaminated soil," *J. Environ. Sci.* Vol. 19, pp. 1120-1124, 2007.
4. I. Levchuk, A. Bhatnagar, M. Sillanpää, "Overview of technologies for removal of methyl tert-butyl ether (MTBE) from water," *Sci. Total Env.* 476-477, 415-433, 2014.
5. N. V. Murthy, A. P. Reddy, N. Selvaraj & C. S. P. Rao, *Aluminum Metal Matrix Nano Composites (Al Mmncs) – Manufacturing Methods: A Review*, *International Journal of Mechanical Engineering (IJME)*, Volume 4, Issue 4, June-July 2015, pp. 29-44
6. P. Roslev, T. Lentz, and M. Hesselsoe, "Microbial toxicity of methyl tert-butyl ether (MTBE) determined with fluorescent and luminescent bioassays," *Chemosphere*, Vol. 120, pp. 284-291, 2014.
7. L. L. P. Lim, and R. Lynch, "Hydraulic performance of a proposed in situ photocatalytic reactor for degradation of MTBE in water," *Chemosphere*, Vol. 82 No. 4, pp. 613-620, 2011.

8. L. L. P. Lim and R. J. Lynch, "In situ photocatalytic remediation of MTBE-contaminated water: Effects of organics and inorganics," *Appl. Catal. A: General*, Vol. 394 No. 1-2, pp. 52-61, 2011.
9. Z. S. Seddigi, A. Bumajdad, S. P. Ansari, S. A. Ahmed, E. Y. Danish, N. H. Yarkandi, et al., "Preparation and characterization of Pd doped ceria-ZnO nanocomposite catalyst for methyl tert-butyl ether (MTBE) photo-degradation," *J. Hazard Mater.* Vol. 264, No. 71-78, pp. 2014.
10. G. Alfonso-Gordillo, C. M. Flores-Ortiz, L. Morales-Barrera, and E. Cristiani-Urbina, "Biodegradation of Methyl Tertiary Butyl Ether (MTBE) by a Microbial Consortium in a Continuous Up-Flow Packed-Bed Biofilm Reactor: Kinetic Study, Metabolite Identification and Toxicity Bioassays," *PLOS ONE*, pp. 1-21, 2016.
11. S. H. Sharidi, "Development of Visible Light-Active Catalyst for MTBE Removal from Ground Water," *Master Thesis, KFUPM*, 2012.
12. H. Sitepu, B. H. O'Connor, and D. Y. Li, "Comparative Evaluation of the March and Generalized Spherical Harmonic Preferred Orientation Models Using X-ray Diffraction Data for Molybdate and Calcite Powders," *J. Appl. Cryst.* Vol. 38 No. 1, pp. 158-167, 2005.
13. H. Sitepu, and S. R. Zaidi, "Structural Refinement of  $Ba_xSr_{1-x}SO_4$  Using X-ray Powder Diffraction Data," *Adv. X-ray Anal.* Vol. 54, pp. 1-8, 2011.
14. H. Sitepu, R. A. Al-Ghamdi, S. R. Zaidi, and S. Shen, "Use of the Rietveld Method for Describing Structure and Texture in XRD Data of Scale Deposits Formed in Oil and Gas Pipelines: An Important Industrial Challenge," *Adv. X-ray Anal.* Vol. 58, pp. 41-50, 2015.
15. H. Sitepu, and R. A. Al-Ghamdi, "Application of the Rietveld Method to the Analysis of XRD Data of Corrosion Deposits Formed in Equipment Parts of Refineries and Gas Plants", *IMPACT: International Journal of Research in Engineering & Technology*, ISSN (P): 2347-4599; ISSN (E): 2321-8843, In Print 2018.
16. D. R. Sellick, D. J. Morgan, and S. H. Taylor, "Silica Supported Platinum Catalysts for Total Oxidation of the Polyaromatic Hydrocarbon Naphthalene: An Investigation of Metal Loading and Calcination Temperature", *Catalysts*, 2015